Available online at www.sciencedirect.com
SCIENCE DIRECT®
Journal of Molecular Catalysis A: Chemical 218 (2004) 81–90
JOURNAL OF MOLECULAR CATALYSIS A: CHEMICAL
www.elsevier.com/locate/molcata

Magnesium-containing mixed oxides as basic catalysts: base characterization by carbon dioxide TPD–MS and test reactions

María A. Aramendía, Victoriano Borau, César Jiménez, Alberto Marinas, José M. Marinas, José R. Ruiz, Francisco J. Urbano*

Department of Organic Chemistry, University of Córdoba, Edf. Marie Curie, Campus de Rabanales, E-14014 Córdoba, Spain

Received 12 January 2004; received in revised form 1 April 2004; accepted 3 April 2004

Abstract

A set of catalysts has been prepared consisting of both pure magnesia and zirconia as well as magnesia-zirconia and magnesia-titania mixed oxides. The basic sites density was determined for all solids from the temperature-programmed desorption of CO_2. Results indicate that magnesia-titania mixed oxides are the most basics followed by magnesia-zirconia, then pure zirconia and, finally, pure magnesia catalysts. Moreover, four test reactions for acid–base characterization of solids were used: 2-methyl-3-butyn-2-ol reaction, propan-2-ol transformation, allylbenzene isomerization and the Aldol condensation of acetone. Although the 2-methyl-3-butyn-2-ol test reaction showed a 100% selectivity to basic products (acetylene and acetone), we were not able to establish a scale of basicity for the catalyst tested. Similar results were obtained for the 2-propanol test reaction. As a final conclusion we can state that although all test reactions gave results according to the basic character of the catalysts, only the Aldol condensation of acetone and allylbenzene isomerization are sensitive enough to establish a basicity scale of the catalyst according to the CO_2 TPD–MS experiments.

Keywords: Basic oxides; Basicity; Magnesia; Zirconia; Magnesia-zirconia; Magnesia-titania; Test reaction

1. Introduction

Magnesia is known to be a typical basic oxide (Hammet constant $H_- = +26.0$), [1,2]. Several studies have been devoted to the modification of its acid–base characteristics in the presence of other species. Therefore, for instance, Aramendía et al. [3] synthesized several $MgO–B_2O_3$ systems, concluding that the density of acid sites increased with the content in boron. On the other hand, the presence of group IA metals, such as sodium, leads to an increase in the basicity of the resulting magnesia [4–6].

Two of the most generalized methods for acid–base characterization of solids are thermal programmed desorption (TPD) of preadsorbed probe molecules and the use of test reactions. As far as TPD studies are concerned, they allow us to get some useful information on the strength of acid and base sites on a catalyst. Ammonia [7,8], pyridine [7–9], 2,6-dimethylpyridine [8–10], CO [11,12] or benzene [13] are some examples of basic probe molecules used in determination of acidity. On the other hand, CO_2 [7,9,14], benzoic [15], acetic [16], trichloroacetic [15], or C–H acids (such as trichloromethane or acetylene) [17] can be utilized for basic characterization of solids.

Regarding test reactions, some of the most frequently used are as follows: (a) dehydration/dehydrogenation processes, such as propan-2-ol [18,19], cyclohexanol [20] and 1-phenylethanol [19]; (b) other alcohol transformations, such as 2-methyl-3-butyn-2-ol [19,21,22]; (c) alkylation of toluene with methanol and formaldehyde [23]; (d) Aldol condensation [24], and retrocondensation [25]; (e) double-bond isomerization [20,26,27,28]; (e) reactions through carbanions different from Aldol condensation, such as Knoevenagel [29–31], or Michael [30,31] condensations.

In a previous work, the synthesis and structural–textural characterization of the magnesium based mixed solids used here was described [32]. In this work, acid–base properties of several magnesia-zirconia and magnesia-titania catalysts are studied by carbon dioxide TPD–MS experiments and

* Corresponding author. Tel.: +34-957-218638; fax: +34-957-212066.
E-mail address: fj.urbano@uco.es (F.J. Urbano).

1381-1169/$ – see front matter © 2004 Elsevier B.V. All rights reserved.
doi:10.1016/j.molcata.2004.04.006

several test reactions. Those catalysts could be further applied in photocalytic processes since ZrO_2 and especially TiO_2 are well known photocatalysts [33–35] or used as support for metals such as palladium in hydrodehalogenation of halogenated compounds [36].

2. Experimental

2.1. Catalysts synthesis and textural–structural characterization

All solids were synthesized by the sol–gel technique, starting from $Mg(NO_3)_2{\cdot}6H_2O$, $ZrOCl_2{\cdot}6H_2O$ (Merck) and TiO_2 (Fluka) and using NaOH as the precipitation agent. The catalysts are named with the symbol of the metals present followed, in the case of mixed oxides, by the atomic Mg/Zr or Mg/Ti ratio, as determined by ICP. Finally "AIR" or "OX" indicate that calcinations were performed either in the air or in the oxygen flow. Details of the catalysts synthesis, together with the textural and structural properties of the solids obtained through physical techniques including TGA-DTA, SEM, XPS, ICP, nitrogen adsorption–desorption isotherms, XRD, FT-Raman, DRIFT and UV-Vis are given in a previous work [32].

2.2. Base characterization of the solids

2.2.1. Temperature-programmed desorption–mass spectrometry experiments

Carbon dioxide (5% CO_2 in Argon) was the probe molecule used to determine the basic properties of the catalysts. The base peak ($m/z = 44$) as well as a secondary one ($m/z = 12$, 10% abundance) were selected to be monitored in the mass spectrometer. Prior to the adsorption of the probe molecule, the catalyst (100 mg) was cleaned by passing an Ar stream (75 mL min^{-1}) at 550 °C for 30 min. The solids were then saturated by passing a CO_2/Ar stream (50 mL min^{-1}) at 50 °C. Subsequently, a pure Ar stream (75 mL min^{-1}) was passed at the saturation temperature for 2 h in order to remove any physisorbed molecules. Once a stable line was obtained, chemisorbed CO_2 was desorbed by heating from saturation temperature up to 900 °C in a programmed fashion, at a rate of 10 °C min^{-1}. The selected peaks were monitored through the whole process. Full details of the TPD–MS method and equipment are given elsewhere [37].

2.2.2. Test reactions

Experiments were carried out in a microcatalytic pulse reactor (1/8 in. i.d. quartz tubular reactor) placed in the injection port of a gas chromatograph (Hewlett Packard Mod. 5890) equipped with a flame ionization detector (FID). The reactor was packed with alternating layers of quartz wool with the catalyst (20 mg) placed between them. Previous to each run, the catalyst was pre-treated in situ in the reactor at 200 °C for 2 h under nitrogen (75 mL min^{-1}). The reactor temperature was then decreased to the lower reaction temperature. Data were collected over a wide range of experimental conditions stated below.

2.2.2.1. 2-Methyl-3-butyn-2-ol (MBOH). MBOH pulse size: 0.5 μL; reaction temperature: 160–350 °C; N_2 flow: 75 mL min^{-1}; analytical column: Supelcowax-10 capillary column (30 m length and 0.20 mm i.d.).

2.2.2.2. Propan-2-ol test reaction. Propan-2-ol pulse size: 0.5 μL; reaction temperature: 260–400 °C; N_2 flow: 75 mL min^{-1}; analytical column: Supelcowax-10 capillary column (30 m length and 0.20 mm i.d.).

2.2.2.3. Condensation of acetone. Acetone pulse size: 0.5 μL; reaction temperature: 300–400 °C; N_2 flow: 75 mL min^{-1}; analytical column: Supelcowax-10 capillary column (30 m length and 0.20 mm i.d.).

2.2.2.4. Allylbenzene double bond isomerization. Allylbenzene pulse size: 0.1 μL; reaction temperature, 160–350 °C; N_2 flow, 75 mL min^{-1}; analytical column: Supelcowax-10 capillary column (30 m length and 0.20 mm i.d.) and SPB-50 (60 m length and 0.25 mm i.d.) capillary column.

In separate experiments, reactions were carried out by using a GC–MS in order to characterize the reaction products of each test reaction.

3. Results and discussion

3.1. Textural and structural characterization

As stated above, the synthesis and textural–structural characterization of the solids used was described in a previous work [32]. The most relevant results are summarized in Table 1.

Pure magnesia solids (Mg-AIR and Mg-OX) are macroporous solids consisting of periclase, the former having a slightly higher surface area. Regarding magnesium-titanium systems, they are mesoporous solids constituted by MgO (periclase) and TiO_2 (anatase) but no mixed phases are observed. The surface area increases as the titanium content decreases. Moreover a surface Ti-enrichment was observed for these catalysts. Finally, MgZr27-OX is a mesoporous solid formed by MgO (periclase) and ZrO_2 (tetragonal phase), the distribution of such crystalline phases being quite homogeneous.

3.2. DRIFT spectra of the catalysts

Figs. 1–3 show the DRIFT spectra of the pure magnesia, magnesia-titania and magnesia-zirconia catalysts, respectively.

Table 1
Summary of the most relevant textural and structural characteristic of the catalysts used in the present work

Catalyst	S_{BET} ($m^2\,g^{-1}$)	Crystalline phases (XRD)	Other comments
Mg-AIR	53	Periclase (MgO)	Macroporous
Mg-OX	47	Periclase (MgO)	Macroporous
MgTi5-OX	52	Periclase (MgO) Anatase (TiO_2)	Mesoporous; surface Ti-enrichment
MgTi19-OX	67	Periclase (MgO) Anatase (TiO_2)	Mesoporous; surface Ti-enrichment
MgTi31-OX	78	Periclase (MgO) Anatase (TiO_2)	Mesoporous; surface Ti-enrichment
MgZr27-OX	74	Periclase (MgO) Tetragonal (ZrO_2)	Mesoporous; regular distribution of Mg and Zr
ZrO2-OX	110	Tetragonal (ZrO_2)	Mesoporous

3.2.1. Pure magnesia catalysts

Fig. 1 shows the DRIFT spectra of the freshly prepared magnesia catalysts (Mg-AIR and Mg-OX), together with an aged Mg-AIR catalyst (1 year). Both, fresh catalysts presents similar spectra. For wavelengths over 3000 cm^{-1}, both isolated hydroxyl groups (above 3700 cm^{-1}) and hydrogen-bridging OH (below 3700 cm^{-1}) are observed [38]. In the region below 2000 cm^{-1}, both Mg–O stretching (1400–1441cm^{-1}) [39]and bands due to adsorbed carbonate [5] appear and, as stated in the previous work, the XPS measurements proved that our samples were carbonated [32]. The main carbonate species in our solids are unidentate carbonates that exhibit bands at 1378 and 1516 cm^{-1} corresponding to the symmetric and asymmetric O–C–O stretching bands.

Fig. 1 also presents the DRIFT spectra of an aged Mg-AIR catalyst, denoted as Mg-AIR(aged). This catalyst exhibits bands around 3611 and 1516 cm^{-1} more intense than those obtained for the fresh catalyst. This is certainly due to re-hydration and carbonation processes occurred during the storage. In this sense, thermal treatment of the aged catalyst (not shown) lead to both water releasing and carbonate decomposition, resulting in a decrease in the corresponding DRIFT bands. It is, therefore, very important from the experimental point of view, to perform a cleaning step previously to the CO_2 adsorption–desorption process or to test any reaction over the magnesium based catalysts.

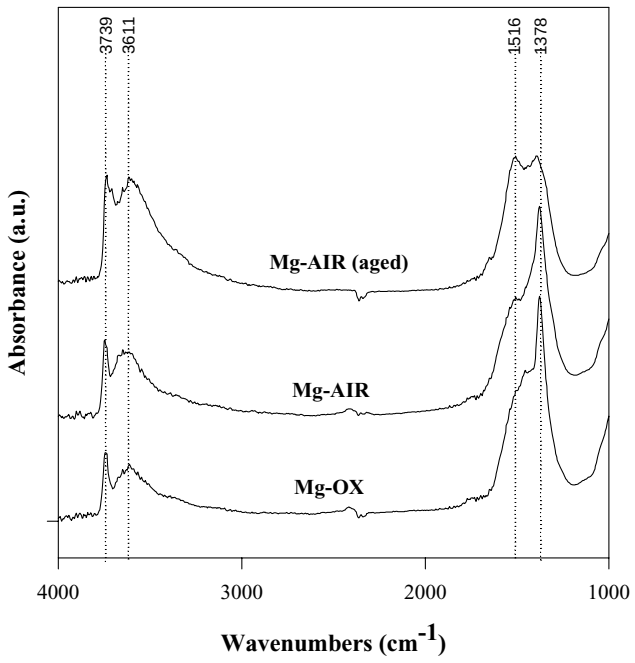

Fig. 1. DRIFT spectra of the magnesium oxides prepared in this work.

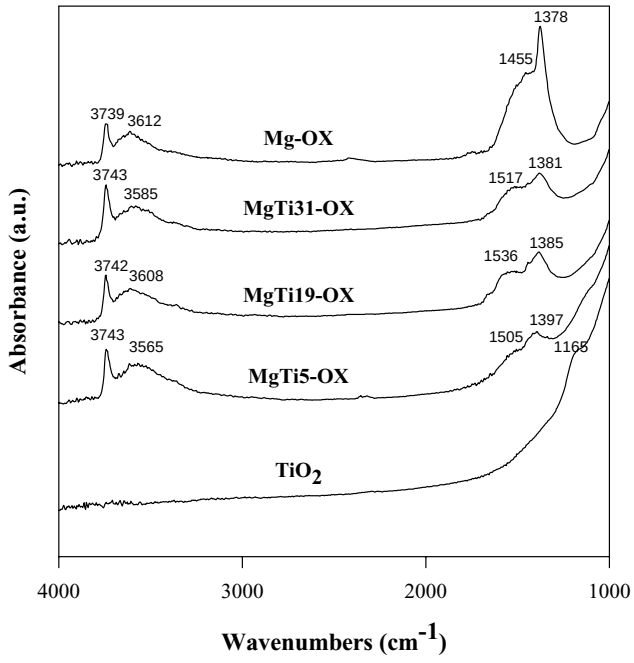

Fig. 2. DRIFT spectra of the magnesiuim-titanium mixed oxides prepared in this work.

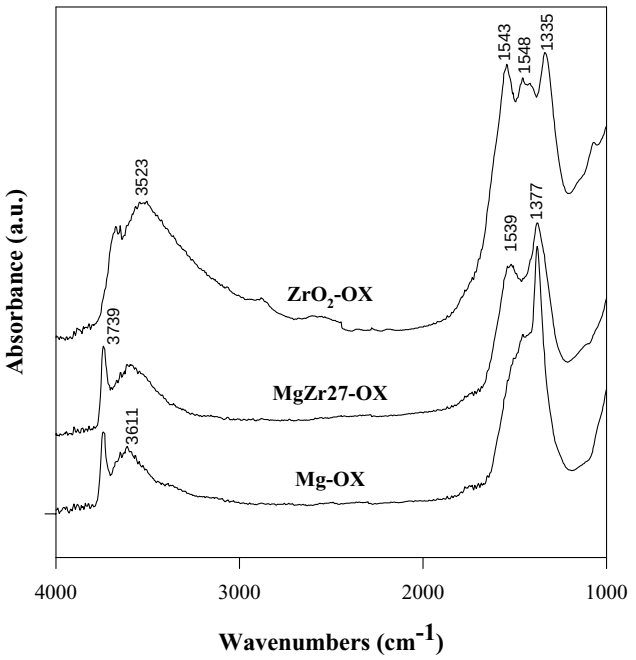

Fig. 3. DRIFT spectra of ZrO_2-OX, Mg-OX and the magnesium-zirconium mixed oxide MgZr27-OX.

3.2.2. Magnesium-titanium systems

Fig. 2 shows the DRIFT spectra for the Mg-Ti systems (MgTi31-OX, MgTi19-OX and MgTi5-OX), together with those of Mg-OX and Fluka TiO_2 calcined at 600 °C and included for comparison. This figure clearly indicates that pure TiO_2 does not present any absorption band due to hydroxyl or carbonate species. Therefore, both isolated (3743 cm^{-1}) and hydrogen bonded hydroxyls (3500–3600 cm^{-1}) are mainly associated to magnesium atoms. Again those bands at 1380 and 1500 cm^{-1}, can be attributed to Mg–O stretching vibration or to the presence of carbonates.

3.2.3. Magnesium-zirconium system

Looking at the DRIFT spectrum of MgZr27-OX (Fig. 3), both isolated and bridging hydroxyl groups can be distinguished at wavelengths coincident to that of pure Mg-OX (3739 and 3611 cm^{-1}). Again, both types of hydroxyl groups seem to be associated to magnesium atoms rather to zirconium. However, unless titania, pure zirconia presents two absorption bands above 3000 cm^{-1}.

In the region below 2000 cm^{-1} bands corresponding to Mg–O and Zr–O stretching vibrations appears together with bands corresponding to surface carbonates. The DRIFT spectra in Fig. 3 indicate that surface carbonates on ZrO2-OX are different than that on Mg-OX or MgZr27-OX.

3.2.4. The nature of surface carbonates

It is well established that the basic character of the solids is associated to carbonation of the surface basic sites. In a previous work [32], XPS experiments revealed that all samples used in this work are carbonated, the extension of which increases with the ageing of the catalysts.

Assignation of the carbonate bands was carried out taking into account the results found in the literature [37,40,38,5] for surface carbonates on magnesium oxides. An attempt at determining the nature of carbonates (whose presence was confirmed by XPS analyses) lead us to point out the existence of unidentate carbonates (1393 and 1526 cm^{-1}). Moreover, such carbonates are mainly due to the presence of magnesia and zirconia but not to titania (Figs. 2 and 3).

3.3. Density and strength distribution of basic sites

In order to achieve a complete characterization of the basic properties of our catalysts, the total number of basic sites, its density and strength distribution were determined by TPD–MS of preadsorbed carbon dioxide.

As revealed by the DRIFT spectra, all catalysts were carbonated and, therefore, a cleaning step prior to the adsorption of CO_2 was performed, as stated in the experimental section.

Figs. 4 and 5 show typical CO_2 TPD–MS profiles obtained for the magnesia-zirconia and magnesia-titania catalysts used in this work. The basic sites were classified according to their different strengths (different carbon dioxide desorption temperature, T_D). Therefore, there are low (T_D below 400 °C), medium (T_D between 400 and 600 °C)

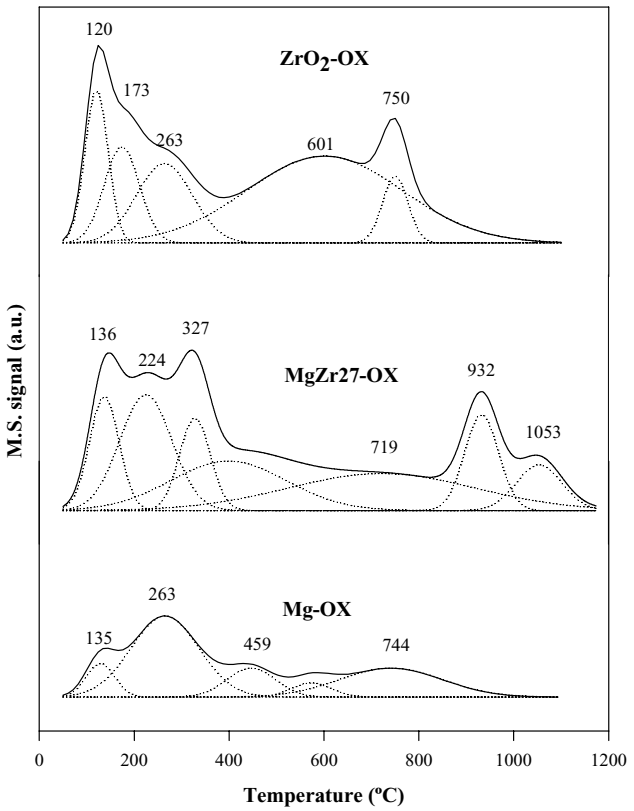

Fig. 4. Carbon dioxide temperature-programmed desorption of ZrO_2-OX, Mg-OX and the magnesium-zirconium mixed oxide MgZr27-OX.

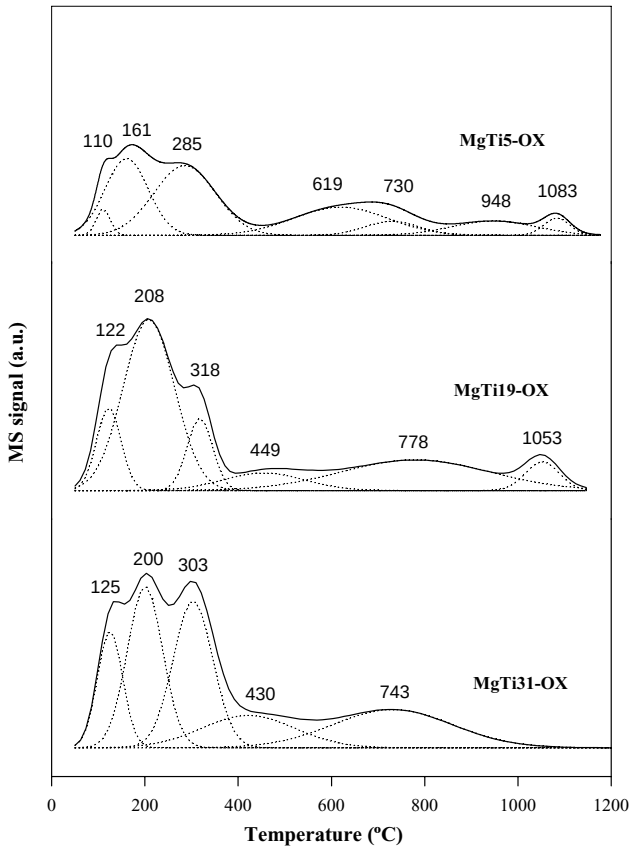

Fig. 5. Carbon dioxide temperature-programmed desorption of the magnesium-titanium mixed oxides MgTi5-OX, MgTi19-OX and MgTi31-OX.

and high strength basic sites (T_D over 600 °C). Note that information obtained from CO_2 desorbed over 600 °C (calcination temperature of the solids) should be carefully considered, since structural transformations could occur on the catalysts. Moreover, since the cleaning step prior to CO_2 saturation was carried out at 550 °C, the high strength basic sites (T_D > 600 °C) were not considered for the discussion in this work.

Pure titania catalyst (Fluka TiO_2 calcined at 600 °C) showed no carbon dioxide desorption peaks in TPD–MS experiments. However, addition of titania to magnesia induces an increase in the density of basic sites. This increase is especially relevant at the medium strength basic sites (T_D between 400 and 600 °C).

On the other hand, if only low and medium strength basic sites (T_D < 600 °C) are compared then magnesia-titania systems are in general, a little bit more basic, than magnesia-zirconia solid and, again, pure magnesia are clearly the less basic solids of the study.

Fig. 6 summarizes the results obtained. This figure presents the basic sites densities for all catalysts calculated from the low strength basic sites (T_D < 400 °C), low plus medium strength basic sites (T_D < 600 °C) and low plus medium plus high strength basic sites (T_D < 900 °C). One of the more remarkable things is the high proportion of carbon dioxide desorbed at temperatures exceeding 600 °C for the MgZr27-OX catalyst (40% of the total CO_2 desorbed).

From these data, we can establish a basicity scale of the catalysts tested, according to the CO_2 desorbed at T_D < 600 °C, as follows:

MgTi31-OX > MgTi19-OX > MgTi5-OX > MgZr27-OX > ZrO2-OX > Mg-OX > Mg-AIR

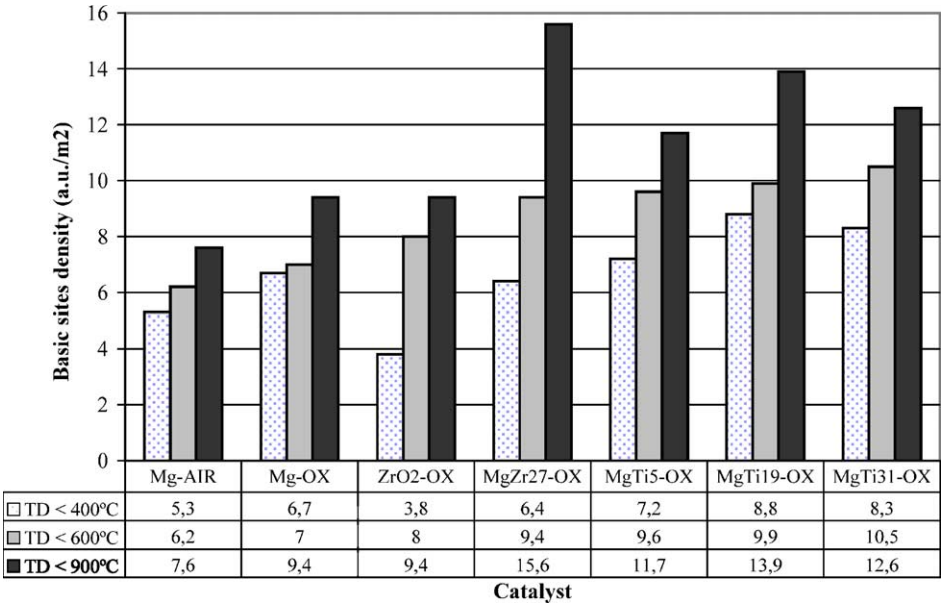

Fig. 6. Surface basicity of the catalysts determined by carbon dioxide TPD–MS. Basic sites densities obtained from the CO_2 desorbed at temperatures below 400, 600 and 900 °C. The catalysts are represented by increasing basicity (from CO_2 desorbed at T_D < 600 °C).

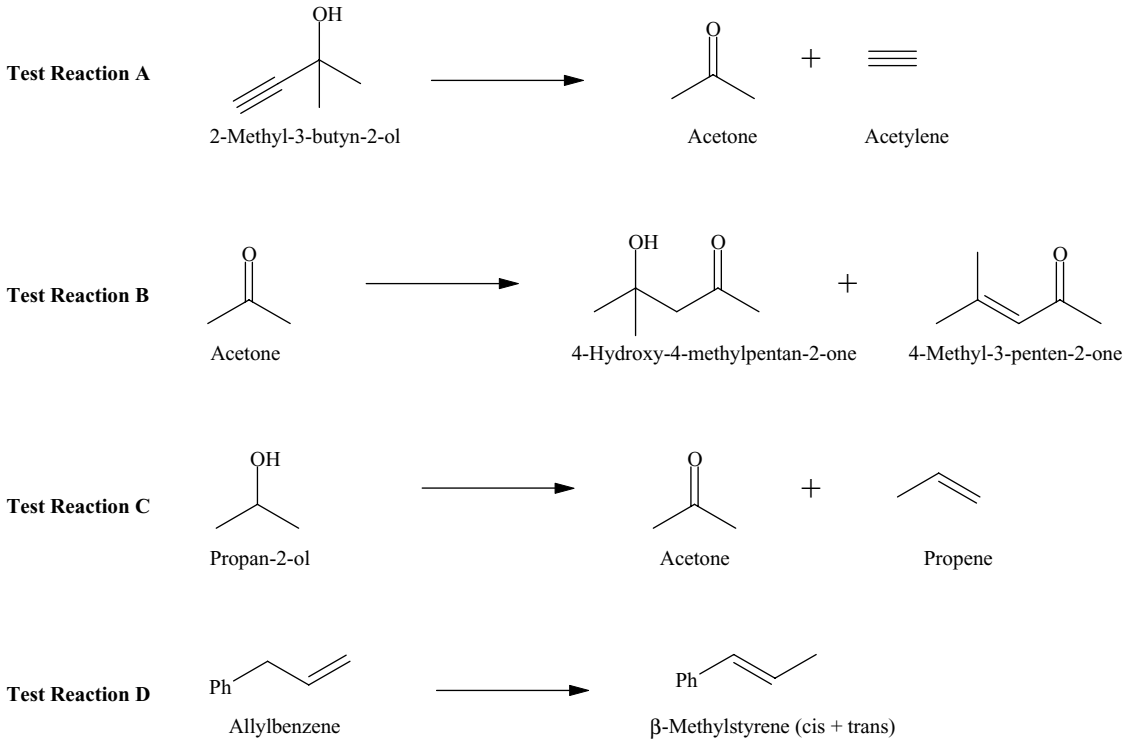

Scheme 1. Test reactions used in this work: (A) 2-methyl-3-butyn-2-ol test reaction; (B) acetone Aldol condensation test reaction; (C) propan-2-ol test reaction; (D) allylbenzene test reaction. The reaction products showed are those mainly obtained over basic catalysts. For the whole reaction paths, see the appropriate references as cited in the text.

Once established this basicity ranking the catalysts were applied to several test reactions in order to investigate whether these processes give results in agreement to the above-mentioned scale.

3.4. 2-Methyl-3-butyn-2-ol (MBOH) test reaction

MBOH test reaction is quite a useful tool in order to have a first idea on the acid–base character of the systems,

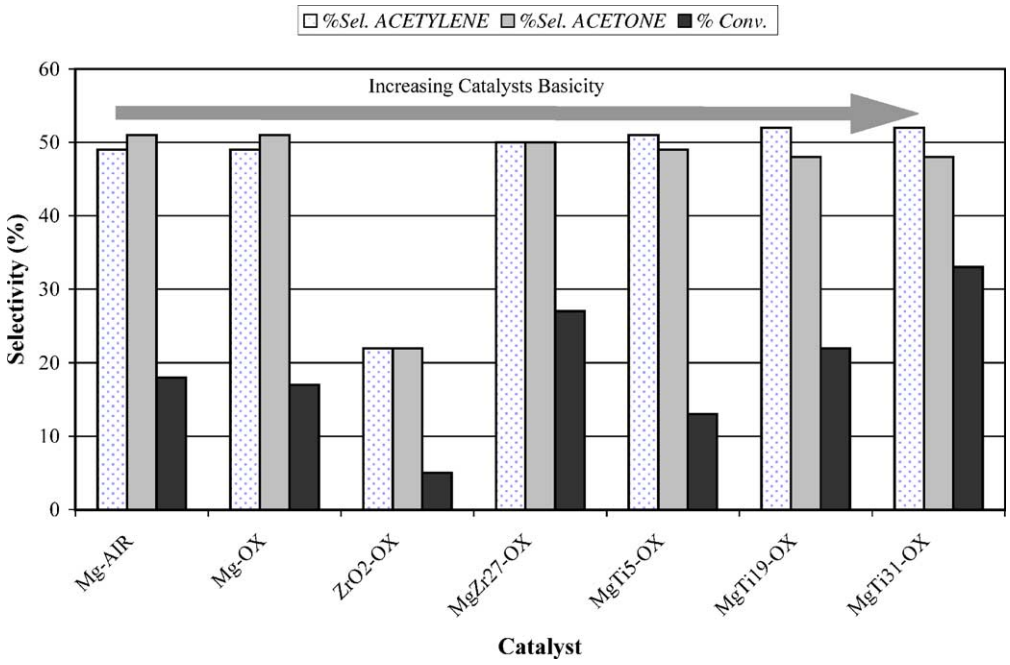

Fig. 7. Molar conversion in the MBOH test reaction at 160 °C. Selectivity to the main products formed over basic sites (acetylene and acetone).

especially of the mixed oxides, since reaction products are different on acid, basic or acid–base pair sites [26,41]. Scheme 1 shows the reaction products obtained after reaction of MBOH over basic sites.

In this sense, all solids but pure zirconia (ZrO2-OX) showed a selectivity close to 100% to the main products formed on basic sites (acetone plus acetylene) throughout the 160–350 °C temperature range (Fig. 7). This figure also presents the MBOH molar conversion at 160 °C, revealing that MgTi31-OX exhibits an enhanced conversion (around 33%) while the rest of the solids give lower conversion levels. Again, the ZrO2-OX catalysts reported the lowest catalytic conversion at the working temperature with only a 5% of the MBOH converted.

This behavior made us think that, although the MBOH test reaction is very useful to classify catalysts in acid, basic or amphoteric [19], is not an efficient test to discriminate catalysts of different basicity such as the solids studied in this work. In fact, we could not carry out any correlation of the results found for this test reaction and the basic strength of the catalysts. There are two catalysts for which the MBOH mole conversion does not fit the basicity scale established from the CO_2 TPD–MS experiments. The first one is the MgTi5-OX that presents a lower MBOH conversion than the pure magnesium catalysts (Mg-OX and Mg-AIR) even when the later are less basic than the former. The second one is the MgZr27-OX that exhibit a quite high conversion for the basicity scale associated to the CO_2 desorbed at $T_D <$ 600 °C. However, it is worth noting here that, although not considered for this ranking, this solid presents a very high population of strong basic sites (up to 40% of the total basic sites are revealed at $T_D >$ 600 °C).

Other authors have also reported some drawbacks for this reaction such as the unfeasibility of this reaction for estimating the nature of very strong bases [26].

According to criteria established by Best and Wojciechowski [42], the optimum performance envelope (OPE) curves (not shown) indicate that acetylene is a primary stable product, whereas acetone is primary unstable. In fact, at high conversions (close to 100%) 4-methyl-3-penten-2-one (mesityl oxide) and 3,5,5-trimethyl-2-cyclohexen-1-one (isophorone) are found in the reaction as secondary products coming from acetone condensation. Some author found these products responsible for the catalyst deactivation by coke formation [43–45].

Since the MBOH test reaction is not suitable to reveal differences between the basic catalysts tested and, as stated above, acetone formed as primary product undergoes Aldol condensation, we decided to check the catalysts against this reaction.

3.5. Condensation of acetone

The acetone Aldol condensation test reaction was tested for all the catalysts in the temperature range of 300–400 °C. The Scheme 1 presents the main reaction products obtained after reaction of acetone over basic catalysts. Results found at 300 and 400 °C are shown in Fig. 8.

The fact that both acid sites and basic sites can catalyze Aldol condensation should be considered. The former implies a process through carbocations whereas carbanions intervene in the latter. However, MBOH test reaction showed that our solids did not present remarkable acidity and,

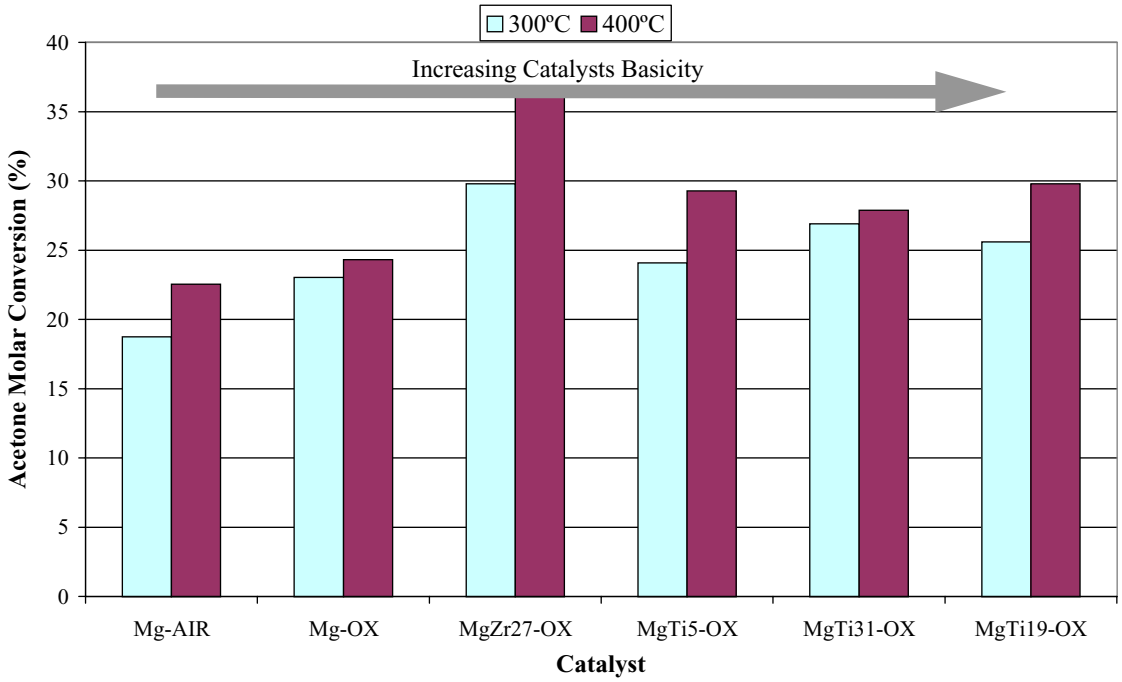

Fig. 8. Molar conversion obtained in the acetone test reaction carried out at 300 and 400 °C over the catalysts studied in this work.

therefore, we can discard the Aldol condensation through carbocations formation.

In this sense, an additional point to take into account is the fact that under our experimental conditions 1,3,5-trimethylbenzene (mesitylene) is hardly obtained from acetone condensation, the major products being mesityl oxide and isophorone. It is known that the more basic a catalyst, the higher the yield of mesityl oxide and isophorone whereas mesitylene (1,3,5-trimethylbenzene) is favored with decreasing basic strength [43–45].

In any case, from Fig. 8 shows that the acetone molar conversion is related to the catalyst basicity. Only the MgZr27-OX catalyst exhibit an enhanced catalytic activity for this reaction exceeding its basicity. We must recall at this point that for the MgZr27-OX catalyst, 40% of the carbon dioxide desorbed was at temperatures exceeding 600 °C, and therefore this must be considered as the reason for the enhanced catalytic activity for the acetone Aldol condensation. For the rest of the solids the higher the catalyst basicity the higher the acetone molar conversion.

3.6. Dehydration–dehydrogenation of propan-2-ol

The transformation of 2-propanol is a widely used test reaction for characterizing both the acidic and basic properties of solids [5,46]. Propan-2-ol undergoes two parallel processes over acid–base catalyst: dehydration to propene and dehydrogenation to acetone (Scheme 1). Thus, the initial rates of dehydration and dehydrogenation have been correlated by many authors with the acidity and basicity, respectively, of the solid used [47], others, however, have found interesting correlations between the ratio of both initial rates and the overall basicity of the catalyst employed [2].

Results found for all the catalysts in terms of selectivity to acetone (dehydrogenation) at 300 and 400 °C, are represented Fig. 9. At a reaction temperature of 300 °C, most of our systems exhibit a selectivity to acetone of 100%. Only the ZrO2-OX and MgTi5-OX catalysts exhibit <100% selectivity (90 and 70%, respectively).

The fact that MgTi5-OX and ZrO2-OX favor the formation of propene could be explained if we assume that both ZrO_2 and TiO_2 are oxides that present acidic character [49]. Therefore, such surface acid sites may be responsible for the loss of selectivity to acetone in the 2-propanol decomposition test reaction.

For a reaction temperature of 400 °C lower selectivity to acetone was obtained for all solids. It has been reported that as temperature increases, the product of dehydration (propane) is favored [48].

In any case, no correlation between activity or selectivity in the 2-propanol test reaction and the surface basic properties of the catalysts was found. As reported, at low reaction temperature (300 °C) most of the catalysts give 100% selectivity to acetone and, therefore, they can not be ranked in terms of basicity nor they can at a reaction temperature of 400 °C.

3.7. Allylbenzene (3-phenyl-1-propene) test reaction

Finally, a double bond isomerization process has also been used for the characterization of the basicity of the catalyst described in this work. This reaction seems to be a more effective means to estimate the nature of strong basic sites

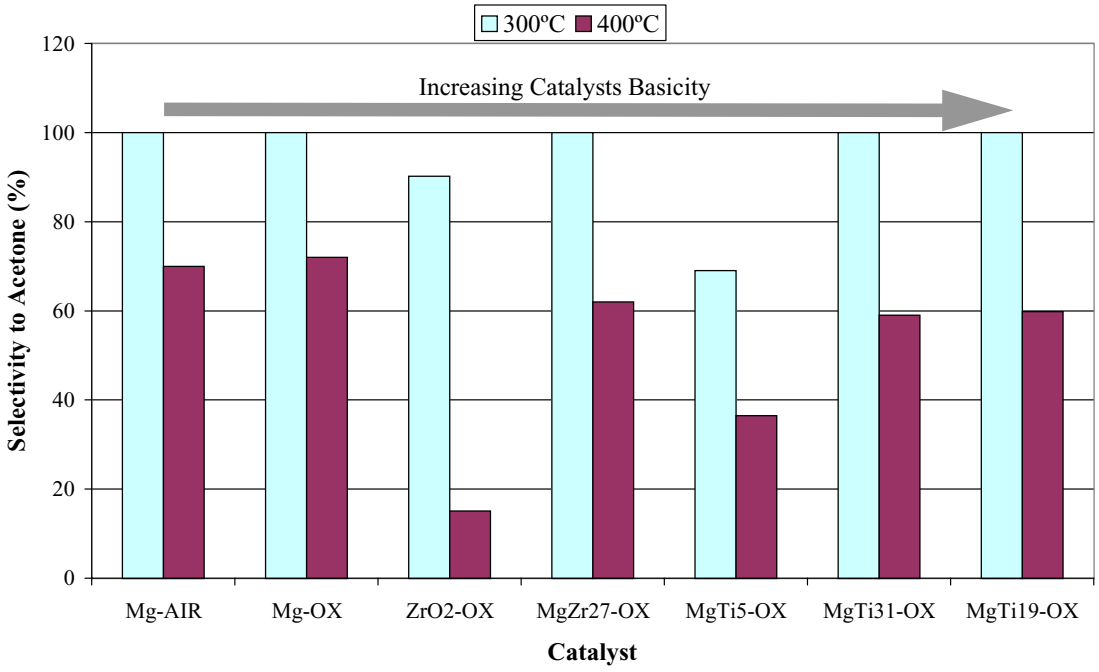

Fig. 9. Propan-2-ol test reaction. Results found for all the catalysts studied in terms of selectivity to acetone at 300 and 400 °C.

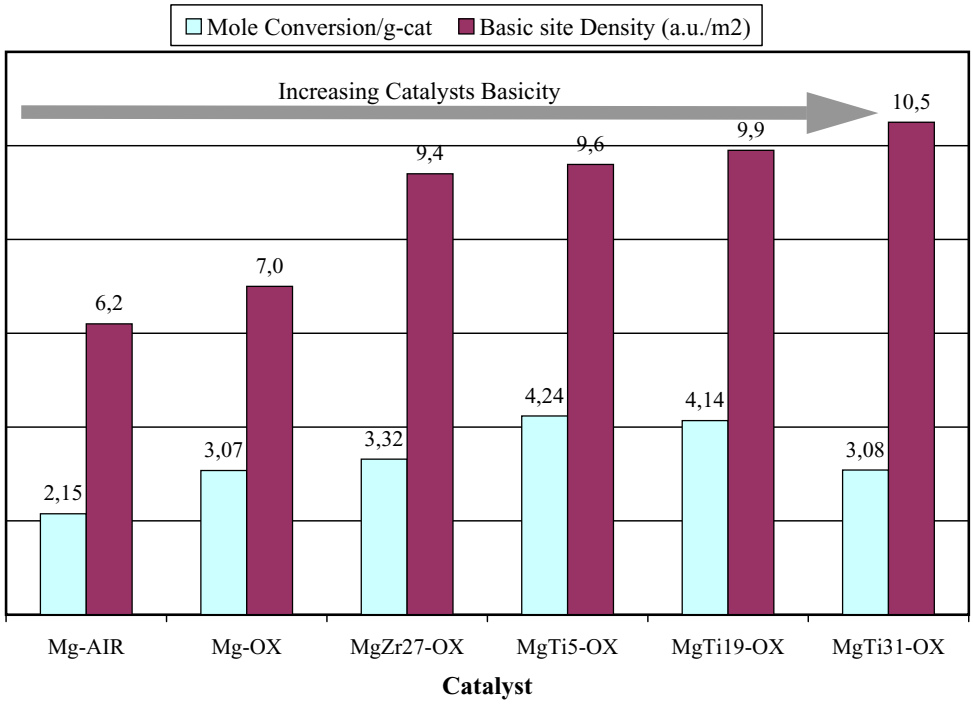

Fig. 10. Allylbenzene test reaction. Mole conversion per gram of catalysts obtained at 250 °C and basic site density obtained from CO_2-TPD (T_D < 600 °C).

than the MBOH one [26]. We carried out the transformation of allylbenzene (3-phenyl-1-propene), since it is known to occurs in homogeneous phase through a carbanionic process [50].

In this sense, as shown in the Scheme 1, isomerization of allylbenzene (3-phenyl-1-propene) could yield *cis* + *trans* β-methylstyrene (1-phenyl-1-propene) through a π-allylic mechanism [28,50]. The driving force of the reaction is the additional stability of the β-methylstyrene due to the conjugation of the olefin bond with the aromatic ring. Usually, the *trans* form is the main product since it is more stable than the *cis*.

This reaction was carried out in the 160–350 °C temperature range. The *trans*/*cis* β-methylstyrene ratio was about 6 for all the catalysts. On the other hand, at high temperatures (over 300 °C) catalyst deactivation, probably due to coke formation, is very important.

Fig. 10 shows the allylbenzene molar conversion (per gram of catalyst) and basic site density for all catalysts, at 250 °C. It can be seen that the allylbenzene mole conversion increases following the basicity of the catalysts as determined from the carbon dioxide temperature-programmed desorption experiments. Only the MgTi31-OX presents an activity result slightly lower than expected.

It is worth noting that the results for the MgZr27-OX fit well the basicity ranking in spite of its large number of strong basic sites (T_D > 600 °C). The reason for this is that double bond isomerization is quite an easy process, not requiring a high basic strength.

4. Conclusions

The above mentioned results allow us to draw the following conclusions.

Basic site density and distribution for all the solids were determined by TPD–MS of CO_2. Following the results obtained the catalysts can be ranked, according to the basic site density, as follows:

MgTi31-OX > MgTi19-OX > MgTi5-OX > MgZr27-OX > ZrO2-OX > Mg-OX > Mg-AIR

In general, magnesia-titania mixed oxides are the more basics followed by magnesia-zirconia mixed oxides. Then, the less basic ones are pure zirconia and pure magnesia. The magnesia-zirconia mixed oxide MgZr27-OX presents a high population of strong basic sites revealed by the desorption of CO_2 at temperatures exceeding 600 °C. However, because of the calcination temperature (600 °C) and cleaning step (at 550 °C) these strong basic sites were not considered for correlations.

According to the 2-methyl-3-butyn-2-ol (MBOH) test reaction, the catalysts studied showed a selectivity close to 100% to products formed on basic sites (mainly acetone and acetylene). Nevertheless, such a reaction did not allow us to establish a scale of basicity.

The detection of some secondary products coming from acetone condensation in MBOH test reaction together with the intrinsic importance of the Aldol condensation of acetone, prompted us to study such a reaction. The acetone

molar conversion is related to the catalyst basicity: the higher the catalyst basicity the higher the acetone molar conversion. The exception was the MgZr27-OX catalyst that presented a catalytic activity exceeding their basic properties, probably due to its strong basic sites (not considered here).

Then, catalysts were tested against the 2-propanol test reaction. Due to their base characteristics most of them exhibited a high selectivity to acetone (dehydrogenation product), especially at lower temperatures. Nevertheless, again, a correlation between obtained results and basic site densities was not possible.

Finally, allylbenzene isomerization test reaction has also been used for the characterization of the basicity of the catalyst described in this work. In general the catalytic activity fits well the basicity ranking of the catalyst tested, with the exception of the MgTi31-OX that presented an activity slightly lower than expected.

As a final conclusion, we can state that although all test reactions gave results according to the basic character of the catalysts, only the Aldol condensation of acetone and allylbenzene isomerization were sensitive enough to establish a basicity scale of the catalyst that matched the carbon dioxide temperature-programmed desorption experiments.

Acknowledgements

The authors gratefully acknowledge the financial support from the *Junta de Andalucía* and the *Ministerio de Ciencia y Tecnología* of the Spanish government in the framework of Project BQU2001-2605 (co-financed with FEDER funds).

References

[1] K. Tanabe, M. Misono, Y. Ono, H. Hattori, Stud. Surf. Sci. Catal. 51 (1989).
[2] A. Gervasini, A. Auroux, J. Catal. 131 (1991) 190.
[3] M.A. Aramendia, V. Borau, C. Jimenez, J.M. Marinas, A. Porras, F.J. Urbano, J. Mater. Chem. 9 (3) (1999) 819.
[4] P. Thomasson, O.S. Tyagi, H. Knozinger, Appl. Catal. A 181 (1) (1999) 181.
[5] V.K. Diez, C.R. Apesteguia, J.I. Di Cosimo, Catal. Today 63 (1) (2000) 53.
[6] F. King, G.J. Kelly, Catal. Today 73 (1–2) (2002) 75.
[7] T. Lopez, R. Gomez, M.E. Llanos, E. Lopez-Salinas, Mater. Lett. 38 (4) (1999) 283.
[8] A.A. Tsyganenko, E.N. Storozheva, O.V. Manoilova, T. Lesage, M. Daturi, J.C. Lavalley, Catal. Lett. 70 (3–4) (2000) 159.
[9] M.A. Aramendia, V. Borau, C. Jimenez, J.M. Marinas, A. Marinas, A. Porras, F.J. Urbano, J. Catal. 183 (2) (1999) 240.
[10] F.M. Bautista, J.M. Campelo, A. Garcia, D. Luna, J.M. Marinas, M.C. Moreno, A.A. Romero, Appl. Catal. A 170 (1) (1998) 159.
[11] D. Spielbauer, G.A.H. Mekhemer, T. Riemer, M.I. Zaki, H. Knozinger, J. Phys. Chem. B 101 (23) (1997) 4681.
[12] S. Coluccia, L. Marchese, andG. Martra, Microporous, Mesoporous Mater. 30 (1) (1999) 43.
[13] F. Arena, R. Dario, A. Parmaliana, Appl. Catal. A 170 (1) (1998) 127.
[14] S. Kus, M. Otremba, A. Torz, M. Taniewski, Appl. Catal. A 230 (1–2) (2002) 263.
[15] P. Kassner, M. Baerns, Appl. Catal. A 139 (1–2) (1996) 107.
[16] J.L. Fung, I.K. Wang, Appl. Catal. A 166 (2) (1998) 327.
[17] S. Huber, H. Knozinger, J. Mol. Catal. A 141 (1–3) (1999) 117.
[18] T. Matsuda, Y. Hirata, H. Sakagami, N. Takahashi, Microporous Mesoporous Mater. 42 (2–3) (2001) 345.
[19] M.A. Aramendia, V. Borau, I.M. Garcia, C. Jimenez, A. Marinas, J.M. Marinas, A. Porras, F.J. Urbano, Appl. Catal. A 184 (1999) 115.
[20] D. Duprez, D. Martin, J. Mol. Catal. A 118 (1) (1997) 113.
[21] H. Lauron-Pernot, F. Luck, J.M. Popa, Appl. Catal. 78 (1991) 213.
[22] G. Zadrozna, E. Souvage, J. Kornatowski, J. Catal. 208 (2) (2002) 270.
[23] T. Yashima, K. Sato, T. Hayasaka, N. Hara, J. Catal. 26 (1972) 303.
[24] G. Zhang, H. Hattori, K. Tanabe, Appl. Catal. 36 (1988) 189.
[25] J.M. Campelo, A. Garcia, D. Luna, J.M. Marinas, Can. J. Chem. 62 (1984) 638.
[26] H. Handa, Y. Fu, T. Baba, Y. Ono, Catal. Lett. 59 (2–4) (1999) 195.
[27] H. Hattori, Appl. Catal. A 222 (1–2) (2001) 247.
[28] M.A. Aramendia, V. Borau, C. Jimenez, A. Marinas, J.M. Marinas, F.J. Urbano, J. Catal. 211 (2) (2002) 556.
[29] I. Rousselot, C. Taviot-Gueho, J.P. Besse, Int. J. Inorg. Mater. 1 (2) (1999) 165.
[30] M.J. Climent, A. Corma, S. Iborra, A. Velty, J. Mol. Catal. A 182–183 (2002) 327.
[31] M.A. Aramendia, V. Borau, C. Jimenez, J.M. Marinas, F.J. Romero, Chem. Lett. (5) (2000) 574.
[32] M.A. Aramendia, V. Borau, C. Jimenez, A. Marinas, J.M. Marinas, J.A. Navio, J.R. Ruiz, F.J. Urbano, Colloids Surf. A 234 (1–3) (2004) 17.
[33] A. Fujishima, T.N. Rao, D.A. Tryk, J. Photochem. Photobiol. C: Photochem. Rev. 1 (1) (2000) 1.
[34] A. Marinas, C. Guillard, J.M. Marinas, A. Fernandez-Alba, A. Aguera, J.M. Herrmann, Appl. Catal. B 34 (3) (2001) 241.
[35] J. Zhang, T. Ayusawa, M. Minagawa, K. Kinugawa, H. Yamashita, M. Matsuoka, M. Anpo, J. Catal. 198 (1) (2001) 1.
[36] M.A. Aramendia, V. Borau, C. Jimenez, J.M. Marinas, F.J. Romero, J. Catal. 183 (1) (1999) 119.
[37] M.A. Aramendia, V. Borau, C. Jimenez, F. Lafont, J.M. Marinas, A. Porras, F.J. Urbano, Rapid Commun. Mass Spectrom. 9 (1995) 193.
[38] W. Ignaczak, W.K. Jozwiak, E. Szubiakiewicz, T. Paryjczak, Polish J. Chem. 73 (4) (1999) 645.
[39] T. Lopez, I. Garcia-Cruz, R. Gomez, Mater. Chem. Phys. 36 (1994) 222.
[40] M.A. Aramendia, V. Borau, C. Jimenez, J.M. Marinas, A. Porras, F.J. Urbano, J. Mater. Chem. 6 (12) (1996) 1943.
[41] U. Meyer, W.F. Hoelderich, J. Mol. Catal. A 142 (2) (1999) 213.
[42] D. Best, B.W. Wojciechowski, J. Catal. 47 (1) (1977) 11.
[43] J.I. Di Cosimo, C.R. Apesteguia, J. Mol. Catal. A 130 (1–2) (1998) 177.
[44] S. Lippert, W. Baumann, K. Thomke, J. Mol. Catal. 69 (1991) 199.
[45] S. Luo, J.L. Falconer, J. Catal. 185 (2) (1999) 393.
[46] T. Lopez, J. Hernandez, R. Gomez, X. Bokhimi, J.L. Boldu, E. Munoz, O. Novaro, A. Garcia-Ruiz, Langmuir 15 (18) (1999) 5689.
[47] D.C. Tomczak, J.L. Allen, K.R. Poeppelmeier, J. Catal. 146 (1994) 155.
[48] J.A. Wang, X. Bokhimi, O. Novaro, T. Lopez, R. Gomez, J. Mol. Catal. A 145 (1–2) (1999) 291.
[49] D. Haffad, A. Chambellan, J.C. Lavalley, J. Mol. Catal. A 168 (1–2) (2001) 153.
[50] F. Joo, E. Papp, A. Katho, Top. Catal. 5 (1998) 113.